ANNUAL REVIEWS

Annual Review of Medicine

Contemporary Application of Cardiovascular Magnetic Resonance Imaging

Yuchi Han,[1] Yucheng Chen,[2] and Victor A. Ferrari[1]

[1]Departments of Medicine (Cardiovascular Division) and Radiology, University of Pennsylvania, Philadelphia, Pennsylvania 19104, USA; email: yuchi.han@uphs.upenn.edu

[2]Departments of Cardiology and Radiology, West China Hospital, Sichuan University, Chengdu, Sichuan, China

Annu. Rev. Med. 2020. 71:221–34

The *Annual Review of Medicine* is online at med.annualreviews.org

https://doi.org/10.1146/annurev-med-041818-015923

Keywords

cardiovascular magnetic resonance imaging, CMR, late gadolinium enhancement, LGE, mapping, nonischemic cardiomyopathy, ischemic heart disease

Abstract

Cardiovascular magnetic resonance imaging (CMR) is a comprehensive and versatile diagnostic and prognostic imaging modality that plays an increasingly important role in management of patients with cardiovascular disease. In this review, we discuss CMR applications in nonischemic cardiomyopathy, ischemic heart disease, arrhythmias, right ventricular diseases, and valvular heart disease. We emphasize the quantitative nature of CMR in current practice, from volumes, function, myocardial strain analysis, and late gadolinium enhancement to parametric mapping, including T1, T2, and T2* relaxation times and extracellular volume fraction assessment.

INTRODUCTION

Cardiovascular magnetic resonance imaging (CMR) has evolved in the last 20 years to become an important noninvasive cardiovascular imaging tool. Its high signal-to-noise ratio using the steady-state free procession (SSFP) cine imaging technique allows precise quantification of chamber size and function. Its velocity encoding, using phase contrast methods, enables quantification of blood flow. Its unique tissue characterization abilities allow identification of fibrosis, fat, iron, edema, and other infiltrative processes that increase extracellular volume. CMR has improved diagnosis and prognosis in patients with ischemic and nonischemic causes of cardiomyopathy. Its lack of radiation makes it ideal in serial imaging to monitor patients on therapy.

In addition to late gadolinium enhancement (LGE), which is a robust technique to detect fibrosis, necrosis, or extracellular protein deposition, recent developments in quantitative tissue characterization using native T1, T2, T2*, and extracellular volume (ECV) mapping have allowed further quantification of diffuse fibrosis/infiltration (elevated native T1), fat deposition (reduced native T1), iron deposition (reduced native T1, T2, or T2*), and edema (elevated T2). ECV mapping is obtained using a formula incorporating pre- and post-contrast myocardial and blood T1 values calibrated by the patient's hematocrit. Pre-contrast (native) T1 and T2 values are field-strength and sequence dependent, so comparing exact values across different vendors and scanners is difficult. ECV is independent of these issues and is more robust when compared across different scanners. First-pass perfusion with gadolinium-containing contrast in conjunction with a stress agent (pharmacologic or exercise) permits detection of significant coronary stenoses. Myocardial strain analysis using algorithms developed for analyzing SSFP cine images has been applied for subclinical disease detection and prognostication. Advanced techniques, such as 4D flow, diffusion tensor imaging, and metabolic imaging, are on the horizon to make CMR the ideal imaging tool for the heart. Deep learning tools are poised to further streamline CMR acquisition, reconstruction, post-processing, and interpretation.

In this review, we focus on CMR methods that are currently available clinically, and on their applications in cardiac diseases that are commonly seen by internists and general cardiologists. **Figure 1** illustrates current CMR methods and several common diseases with their morphologic findings using cine imaging, LGE, parametric tissue mapping, myocardial perfusion, and flow quantification.

Cardiovascular magnetic resonance imaging (CMR): overall term for a vast collection of sequences and techniques to image the heart using magnetic resonance imaging

Steady-state free procession (SSFP): an imaging sequence to evaluate cardiac morphology and function with high myocardium–to–blood pool contrast

Late gadolinium enhancement (LGE): bright areas indicating fibrosis and necrosis detected 10–30 min after injection of gadolinium-containing contrast

T1: a time constant of longitudinal magnetization relaxation, obtained by sampling the tissue longitudinal relaxation curve using different sequences

T2: a time constant of transverse magnetization decay, obtained by sampling the tissue transverse relaxation curve

T2*: an observed time constant of transverse magnetization decay, strongly influenced by inhomogeneity of the main magnetic field, which can occur due to susceptibility-induced field distortions produced by iron in the tissue

CLINICAL APPLICATIONS IN NONISCHEMIC CARDIOMYOPATHY

Dilated Cardiomyopathy

Dilated cardiomyopathy (DCM) is a heterogenous disease characterized by left ventricular (LV) dysfunction associated with LV or biventricular dilatation. With its advantages of greater accuracy than echocardiography in measuring LV volume, function, and mass, and in characterizing myocardial tissue, CMR has played a critical role in the diagnosis, risk stratification, treatment monitoring, and prognosis of DCM patients. Ischemic cardiomyopathy (subendocardial to transmural LGE in a coronary artery distribution) can be ruled in or out using LGE patterns, while sarcoidosis and myocarditis can be identified by focal epicardial and/or mid-myocardial involvement. The pathological changes of dilated cardiomyopathy can manifest as focal septal mid-wall LGE, which can be identified in approximately 30% of patients (1), or myocardial interstitial fibrosis, which can be determined by myocardial native T1 and ECV mapping (2). While the presence of LGE portends a worse prognosis in DCM patients (3), the clinical outcomes could also be affected by the extent, location, and pattern of LGE (4). ECV adds incremental prognostic value to LGE and native T1 mapping (5). Recovery from LV dilation and systolic dysfunction, also known as reverse remodeling, can be observed in some patients treated with optimal medical therapy

a Morphology

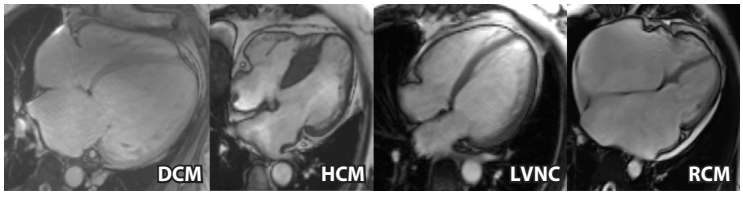

b Late Gadolinium enhancement

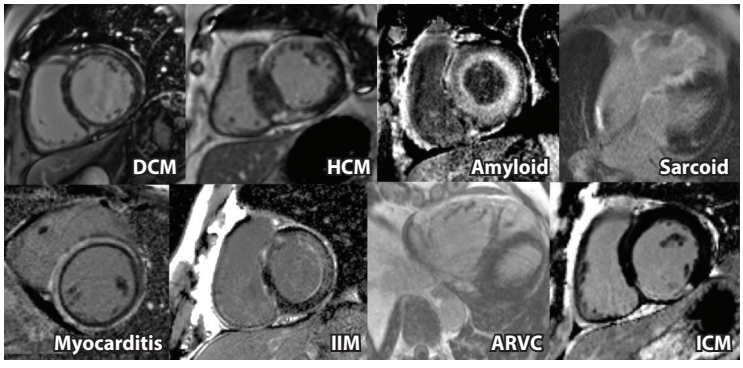

c Parametric mapping

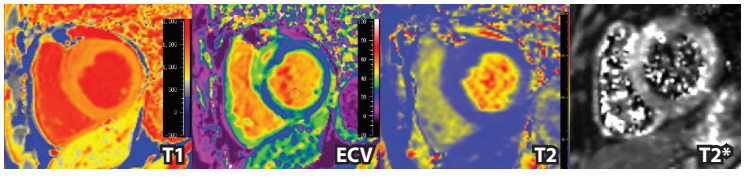

d Perfusion

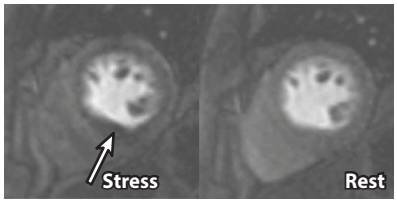

e Valvular regurgitation quantification

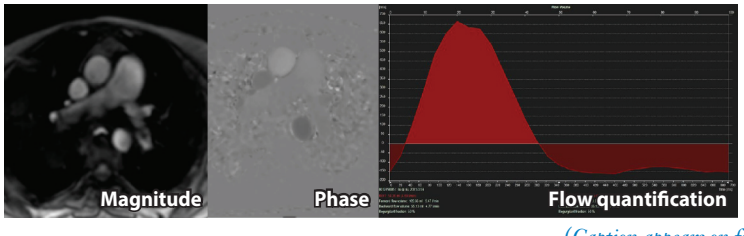

(*Caption appears on following page*)

Figure 1 (*Figure appears on preceding page*)

Contemporary cardiovascular magnetic resonance imaging (CMR) techniques with illustrative examples. (*a*) Morphological cine imaging can identify diseases such as dilated cardiomyopathy (DCM), hypertrophic cardiomyopathy (HCM), left ventricular noncompaction (LVNC), and restrictive cardiomyopathy (RCM). (*b*) Late gadolinium enhancement (LGE) examples demonstrate typical LGE patterns in DCM, HCM, cardiac amyloid, sarcoidosis, myocarditis, idiopathic inflammatory myopathy (IIM), arrhythmogenic right ventricular cardiomyopathy (ARVC), and ischemic cardiomyopathy (ICM). (*c*) Parametric methods include native T1, T2, T2*, and extracellular volume (ECV) mapping. (*d*) Myocardial perfusion with adenosine stress identifies areas of ischemia (*arrow*) when compared to rest perfusion images. (*e*) Valvular regurgitation volume is quantified directly in aortic regurgitation using velocity encoded phase contrast technique. The acquisition includes magnitude images and phase images. Flow quantification is obtained by post-processing the phase images with a region of interest in the ascending aorta and integrating the blood flow over time.

(6). The presence of LGE and increased ECV may be associated with poor treatment response (7). In new-onset idiopathic DCM, an increased myocardial T2 value suggests that inflammation may be present and is a potential cause of the DCM (8). While myocardial strain can be obtained in echocardiography using speckle tracking, CMR can also assess ventricular strain using feature tracking, with longitudinal strain demonstrating the best prognostic value (9). New geometric parameters, such as the 3D-spherical index, have demonstrated better prognostic value than LV ejection fraction (EF) in DCM patients (10). A recent study showed that symptoms can recur in patients with DCM after initial recovery with optimal medical treatment (11). This suggests that our understanding of myocardial recovery in DCM patients is insufficient, and CMR can help us to further explore the mechanism of reverse remodeling.

Hypertrophic Cardiomyopathy

Hypertrophic cardiomyopathy (HCM) is an autosomal dominant hereditary disease. With the advancement of genetic testing (12), the current prevalence of 1:500 in the general population may be an underestimate. CMR can provide comprehensive information for the diagnosis and treatment of HCM, including assessment of focal or global myocardial thickening, abnormal valves and blood flow, and myocardial histopathological changes (13). Although HCM is phenotypically heterogeneous, CMR offers precise phenotypical description of areas of focal hypertrophy. Native T1 and ECV mapping have helped to detect early myocardial abnormalities in mutation carriers without myocardial hypertrophy, suggesting that myocardial interstitial fibrosis is an early feature of HCM (14, 15). Recent studies have found that focal and interstitial fibrosis in HCM may progress over years, and such changes may be associated with myocardial remodeling and poor prognosis (16). Additionally, the presence of basal inferoseptal crypts in the LV myocardium may be helpful in distinguishing disease-causing HCM mutations from those with genotype-negative HCM (17). Elongation of mitral valve leaflets is common in HCM and is also found in mutation carriers without a typical HCM phenotype (18).

Extracellular volume (ECV): a parameter obtained from pre- and post-contrast T1 mapping of the myocardium and blood pool, adjusted for patient's hematocrit

Myocardial strain: myocardial regional function measured by local tissue deformation. Myocardial feature tracking and other registration techniques allow simplified analysis using steady-state free procession images, which can be easily performed retrospectively

Native T1 mapping could help to differentiate HCM (elevated T1) from athlete's heart (normal T1) and hypertensive heart disease (mildly elevated T1) (15, 19). Additionally, the differences in native T1 and ECV between rare diseases and HCM can differentiate cardiac hypertrophy from disorders such as transthyretin amyloidosis (highly elevated T1 and ECV) (20) or Fabry disease (decreased T1) (21).

A recent meta-analysis showed significant predictive value in LGE for sudden cardiac death prediction in HCM (adjusted hazard ratio 1.36/10% LGE; 95% confidence interval 1.10–1.69; $p = 0.005$) (22). Decreased right ventricular (RV) EF measured by CMR also suggests a poor prognosis in HCM (23). Several additional CMR imaging markers have demonstrated independent prognostic value, such as decreased LV strain by feature tracking, decreased left atrial longitudinal

strain, elevated T2 signal, and LGE texture features in HCM (24–27). Future studies are needed to create a risk stratification model incorporating multiple clinical and CMR prognosticators.

Infiltrative or Inflammatory Cardiomyopathies

Systemic diseases that can affect the heart include amyloidosis, sarcoidosis, rheumatologic diseases such as rheumatoid arthritis, systemic sclerosis, idiopathic inflammatory myopathy, and vasculitis. Other systemic disorders include endocrine and metabolic diseases such as hemochromatosis, hyper or hypothyroidism, carcinoid, pheochromocytoma, Anderson-Fabry disease, and systemic infectious disease such as human immunodeficiency virus. Occasionally, isolated cardiac presentations are well described in amyloid and sarcoid. The cardiac manifestations of these diseases can be quite varied, including myocardial inflammation, vasculitis or coronary artery disease or dissection causing infarction, valvular disease, and different patterns of myocardial fibrosis. We illustrate here a few examples with typical findings on CMR.

Cardiac amyloidosis. Global subendocardial LGE is a characteristic finding with 88% sensitivity and 90% specificity in the diagnosis of cardiac amyloidosis (28). ECV and native T1 values are correlated with serum biomarkers and can increase significantly, even in patients without significant LV hypertrophy or typical LGE (29). Based on myocardial segmental strain and ECV analysis, the basal ventricular myocardium is found to be affected earlier and more severely with amyloid infiltration (30, 31). The relative apical sparing can be used to differentiate between cardiac amyloidosis and other forms of LV hypertrophy. Recently, a T2 mapping study also showed significantly elevated T2 in light-chain compared to transthyretin cardiac amyloidosis (32).

A meta-analysis that included 425 patients with amyloidosis in seven studies showed significantly higher all-cause mortality in LGE-positive patients (33). LGE-based semiquantitative analysis can further differentiate patients' prognoses (34). ECV and LGE pattern can improve the risk prediction beyond the Mayo staging system (35). Although cardiac amyloidosis predominantly affects the LV, RV volume and RV dysfunction are better prognosticators (36). Recent studies have also shown that CMR-based radial, longitudinal, and circumferential strains are independent predictors of patients with light-chain amyloidosis (37).

Cardiac sarcoidosis. Cardiac sarcoidosis can be part of a multi-system disease with infiltration of noncaseating granulomas. When the heart is involved, complete atrioventricular block, ventricular tachycardia, heart failure, and sudden death can occur. Currently, the Japanese Ministry of Health and Welfare (JMHW) diagnosis of sarcoidosis is an international standard and is dependent on histopathological findings on biopsy. Typical myocardial involvement manifests in CMR as a noncoronary distribution of segmental wall motion abnormality and delayed enhancement with elevated T2 values (38). CMR myocardial quantification can detect early myocardial abnormalities of sarcoidosis by elevated T1, T2, and ECV values compared to normal controls (39). The values of the area under the curve for T1 and T2 in patients with sarcoidosis as compared to normal controls were 0.96 and 0.89, respectively, which were significantly higher than the JMHW criteria (0.61) and Heart Rhythm Society criteria (0.67) (40). After treatment, the T1 and T2 values were significantly lower, while the untreated patients showed no change in T1 and T2 values, suggesting that T1 and T2 mapping techniques can be used for early detection and monitoring of cardiac sarcoidosis (40).

Delayed enhancement is an important predictor of cardiac events in LGE-positive patients with sarcoidosis, who were 9 times more likely to have adverse events than LGE-negative patients (41). Among sarcoidosis patients with an LVEF greater than 50%, LGE-positive patients had a

significantly higher risk of death or ventricular tachycardia than LGE-negative patients (4.9 versus 0.2%, $p < 0.01$). In a meta-study involving 10 studies, LGE-positive patients were 3 times more likely to have all-cause mortality than LGE-negative patients, and the risk of arrhythmia and all-cause mortality was nearly 11 times higher (42).

Iron overload cardiomyopathy. Iron deposition in the myocardium can lead to cardiac dysfunction and heart failure, commonly found in transfusion-dependent thalassemia and primary iron excess in hereditary hemochromatosis. The current tool for quantitative evaluation of cardiac iron deposition is T2* mapping; myocardial T2* < 20 ms suggests myocardial iron deposition, and myocardial T2* < 10 ms suggests severe myocardial iron deposition. An international survey of 3,095 thalassemia patients in 27 centers showed that T2* < 10 ms was a predictor of heart failure and death (43). Cardiac T2* mapping of iron deposition can be used for risk stratification and evaluation of treatment efficacy (44). The implementation of screening programs in the United Kingdom using T2* CMR has dramatically improved the natural history of iron overload cardiomyopathy with significantly increased survival (45). Recently, CMR T1 and T2 mapping have been shown to have excellent sensitivity and specificity to detect iron overload (46).

Arrhythmogenic Right Ventricular Cardiomyopathy

Arrhythmogenic RV cardiomyopathy (ARVC) is a genetic cardiomyopathy characterized by fibrofatty replacement of predominantly the RV myocardium, which predisposes patients to RV dysfunction and life-threatening ventricular arrhythmias. Although the estimated prevalence in the general population is only 1:5,000, ARVC is one of the most common causes of death in young people and athletes (47). Quantitative CMR criteria for RV size and global function, in addition to qualitatively assessed regional RV dysfunction, are included in the 2010 modified task force criteria for ARVC diagnosis (48). Additionally, structural abnormalities in ARVC have been shown to be preferentially located in the epicardial subtricuspid region, whereas the RV apex and endocardium are relatively spared (49). RV LGE has been observed in up to 88% of patients (50) and has been shown to be closely related to arrhythmia events (51).

Left Ventricular Noncompaction Cardiomyopathy

LV noncompaction cardiomyopathy (LVNC) is characterized by extensive LV trabeculations with a thin, compacted myocardial layer and potential risk of heart failure, thromboembolism, and malignant arrhythmias (52). There is a lack of uniform diagnostic criteria for LVNC. CMR has the advantage of a high contrast ratio between the myocardium and blood pool and plays a growing role in the diagnosis of LVNC (52, 53). However, the degree of LV trabeculation does not show greater prognostic value than LV dilation, systolic dysfunction, and the presence of LGE (54). Additionally, the degree of trabeculation was not found to be associated with cardiovascular outcomes in DCM patients (55).

CLINICAL APPLICATIONS IN ISCHEMIC HEART DISEASE

Stress Testing

CMR stress testing is performed either with vasodilators (adenosine, regadenoson, or dipyridamole) or by increasing myocardial demand using dobutamine or exercise (56). The safety and feasibility of stress CMR have been confirmed in patients with coronary artery disease (CAD) (57). Meta-analysis showed that the sensitivity and specificity of stress CMR to diagnose CAD

were very high (at 3T, sensitivity of 90% and specificity of 79%) (58). Stress-induced wall motion abnormalities and perfusion defects demonstrated good sensitivity and specificity for the diagnosis of CAD (59). Subsequent studies have confirmed stress CMR's prognostic value in diagnosing coronary artery disease (60, 61). Stress CMR reduced unnecessary revascularization in patients with acute chest pain (62).

Exercise stress CMR has been limited in clinical use due to the need of MRI-compatible equipment. The feasibility of exercise CMR has been demonstrated in normal volunteers and in patients suspected of ischemic heart disease (63, 64). Subsequent studies have shown that stress CMR can be used to predict myocardial infarction (MI), cardiac death, and hospitalization in patients with unstable angina and known or suspected CAD (65).

Viability Evaluation

The current goal of assessing myocardial viability is to analyze the proportion of viable myocardium in patients in order to determine which patients are most likely to benefit from revascularization. Evaluating myocardial viability by CMR includes three main assessments: (*a*) LV end-diastolic wall thickness (EDWT) at rest $\geq$5.5–6.0 mm; (*b*) LV wall hyperenhancement (LGE-CMR) < 50%; and (*c*) change of ventricular wall thickness with low-dose dobutamine (LDD) stress CMR > 2 mm (66). Using single-photon-emission computed tomography (SPECT) as the gold standard for viability, the sensitivity of EDWT, LGE-CMR, and LDD was 94%, 93%, and 84%, respectively, but the specificity was lower. Using the recovery of contractile function six months after coronary artery bypass graft as the gold standard, the sensitivity of LGE-CMR, EDWT, LDD, and SPECT was 99%, 96%, 84%, and 86%, respectively (67). This suggests that CMR may be better than SPECT imaging in assessing myocardial viability. A meta-analysis showed that the relative sensitivity of predicting LV segmental systolic function recovery after revascularization was LGE-CMR > EDWT > LDD and the relative specificity was LDD > LGE-CMR > EDWT (68). Dysfunctional viable myocardium with LGE-CMR is an independent predictor of mortality in patients with ischemic LV dysfunction without revascularization (69). A recent study found that native T1 mapping could also distinguish between irreversible and reversible myocardial injury in patients with ST-segment elevation MI and that T1 value had a strong correlation with LV remodeling (70).

Coronary Artery Imaging

Coronary MR angiography can be performed using the SSFP technique, and some studies have demonstrated feasibility; however, the accuracy and sensitivity are limited as compared to computed tomography (CT) angiography (71). Recent advances in CMR techniques, such as noncontrast T1-weighted imaging and molecular imaging techniques, demonstrated that the lipid core or hemorrhage in coronary plaque were indictors for unstable plaque (72, 73). In clinical settings, such as assessing for coronary aneurysm or congenital anomalous coronary origin, and in patients with contraindication to iodinated contrast, coronary MR angiography can be useful.

Myocardial Infarction with Nonobstructive Coronary Arteries

Myocardial infarction with nonobstructive coronary arteries (MINOCA) is an emerging subgroup of myocardial injury, accounting for nearly 5–10% of acute MI patients with unfavorable prognosis (74). A combination of cine, T2-weighted, and LGE imaging can be helpful in identifying MINOCA in patients with elevated cardiac biomarkers (75). CMR changed the diagnosis in almost 50% of patients and led to changes in clinical management and correct prediction of the

infarct-related artery in some patients (76). In a group of patients with aborted sudden cardiac death, CMR helped to identify occult MI in individuals with normal coronary arteries (77).

ARRHYTHMIA EVALUATION

Atrial fibrillation (AF) is the most common sustained arrhythmia, and its treatment continues to be challenging. In the Multi-Ethnic Study of Atherosclerosis (MESA), left atrial volume enlargement as well as decreased left atrial functional parameters increased the risk for incident AF (78). There is evidence that left atrial LGE, indicating atrial fibrotic changes, may precede AF onset in a significant proportion of individuals (79). The results of several studies suggest that the total scar burden and location play important roles in the development of arrhythmia recurrences after AF ablation. Pulmonary vein reconnection is considered the main cause for AF ablation failure, and discontinuities in previous ablation sets are a common underlying mechanism for resumption of conduction. CMR may be able to guide repeat pulmonary vein isolation procedures in AF ablation by identifying and localizing gaps and may reduce procedure time (80).

Ventricular tachycardia (VT) is a major cause of sudden cardiac death, especially in patients with structural heart disease. CMR is considered the gold standard for imaging of the VT substrate (81) to provide guidance for VT ablation (82). The future of complex VT ablation lies in CMR-guided interventions in which the ablation takes place in the scanner, where the substrates can be visualized in real time. Recently, patients with isthmus-dependent atrial flutter were successfully treated with CMR-guided cavotricuspid isthmus ablation (83). It is a first step toward real-time CMR-guided complex ablation procedures.

RIGHT VENTRICLE AND PULMONARY ARTERY HYPERTENSION EVALUATION

The RV is difficult to evaluate using echocardiography due to its retrosternal location and complex geometry; thus, CMR is the gold standard for the assessment of RV size and function. RV size and function are altered by diseases affecting the preload (left to right shunts, tricuspid regurgitation, and pulmonic regurgitation), afterload (increased pulmonary vascular resistance in pulmonary hypertension and pulmonic stenosis), and intrinsic myocardium of the RV (ARVC). The ratio of RV to LV end-diastolic volume can better detect RV enlargement than using indexed RV end-diastolic volume alone (84).

Left to right shunts can be measured using velocity-encoded phase contrast imaging, which allows for Qp:Qs shunt calculations noninvasively. Tomographic structural imaging with MR angiography can identify atrial septal defects and partial anomalous pulmonary venous return.

Pulmonary arterial hypertension (PAH) is a disease of the pulmonary vasculature, but the related mortality and morbidity depend on RV function. CMR can assess RV–pulmonary artery coupling, which reflects the relationship between myocardial contractility and pulmonary vascular compliance. RV–pulmonary artery coupling derived from CMR was shown to be in good agreement with invasive right heart catheterization measurements and was prognostic (85). CMR can evaluate RV tissue remodeling by LGE and T1 mapping. The LGE of PAH occurs mainly in the RV insertions, and its presence reflects disease progression and poor prognosis (86). The native T1 value of RV insertion is also closely related to the severity of the disease (87). Dynamic monitoring of RV remodeling to follow therapeutic response is important in understanding the effectiveness of PAH treatment.

CMR can also noninvasively assess pulmonary vascular hemodynamics via phase contrast sequences. Pulmonary artery stiffness might be helpful for early diagnosis of PAH (88), and increased

pulmonary artery stiffness can be associated with increased mortality (89). Pulmonary vortex intervals obtained by 4D flow can indirectly assess pulmonary artery pressure and identify patients with PAH and borderline PAH (90).

VALVULAR HEART DISEASE EVALUATION

Echocardiography is the predominant imaging modality for the assessment of heart valve disease. CMR can complement echocardiography in the quantitative evaluation of valvular regurgitation volumes and in the assessment of changes in myocardial tissue as sequelae of valve disease.

The use of CMR in aortic stenosis assessment includes anatomical assessment of the aortic valve and aortic root; quantification of LV volume, mass, and function; and calculation of stenotic jet velocity (91). In patients with aortic stenosis, LGE and T1 mapping can be used to identify focal and diffuse fibrosis, which has prognostic implications (92, 93).

CMR can also accurately assess the structure of the aortic root, which is important for annular sizing in patients who are candidates for transcatheter aortic valve replacement (TAVR) but who cannot undergo contrast CT imaging (94). Aortic regurgitation can be directly measured using CMR velocity-encoded phase contrast imaging. In post-operative TAVR paravalvular regurgitation assessment, CMR can serve as an alternative to echocardiography, especially since grading paravalvular regurgitation by using conventional echocardiography techniques can be challenging (95).

The current guidelines recommend the use of CMR to assess the severity of mitral regurgitation when echocardiographic assessment is not satisfactory (96). CMR mitral regurgitation volume assessment, using the difference of LV stroke volume from cine imaging and aortic forward flow volume from phase contrast imaging, has high reproducibility (97). Recent studies have indicated that CMR-derived assessment of primary mitral regurgitation can better identify patients with severe disease and adverse outcome than the guideline-recommended integrative approach by echocardiography (98). Substrate evaluation by CMR also has determined papillary muscle fibrosis to be associated with arrhythmogenic mitral valve prolapse (99).

CMR has been widely used in patients with pulmonary regurgitation after tetralogy of Fallot repair to determine the timing and prognosis for pulmonic valve replacement (100).

CONCLUSION

CMR is a quantitative cardiovascular imaging tool that is versatile and avoids the risk of radiation. It is uniquely suited for the quantitative evaluation and monitoring of cardiac structure and myocardial substrate. Its contemporary application encompasses virtually all aspects of cardiovascular diseases. With rapid advancement in acquisition and post-processing, CMR is the deep-phenotyping tool of choice for the heart in the era of precision medicine.

DISCLOSURE STATEMENT

The authors are not aware of any affiliations, memberships, funding, or financial holdings that might be perceived as affecting the objectivity of this review.

LITERATURE CITED

1. Mahrholdt H, Wagner A, Judd RM, et al. 2005. Delayed enhancement cardiovascular magnetic resonance assessment of non-ischaemic cardiomyopathies. *Eur. Heart J.* 26:1461–74
2. Nakamori S, Dohi K, Ishida M, et al. 2018. Native T1 mapping and extracellular volume mapping for the assessment of diffuse myocardial fibrosis in dilated cardiomyopathy. *JACC Cardiovasc. Imag.* 11:48–59

3. Becker MAJ, Cornel JH, van de Ven PM, et al. 2018. The prognostic value of late gadolinium-enhanced cardiac magnetic resonance imaging in nonischemic dilated cardiomyopathy: a review and meta-analysis. *JACC Cardiovasc. Imaging* 11:1274–84
4. Halliday BP, Baksi AJ, Gulati A, et al. 2019. Outcome in dilated cardiomyopathy related to the extent, location, and pattern of late gadolinium enhancement. *JACC Cardiovasc. Imaging* 12:1645–55
5. Vita T, Grani C, Abbasi SA, et al. 2019. Comparing CMR mapping methods and myocardial patterns toward heart failure outcomes in nonischemic dilated cardiomyopathy. *JACC Cardiovasc. Imaging* 12:1659–69
6. Gupta A, Goyal P, Bahl A. 2014. Frequency of recovery and relapse in patients with nonischemic dilated cardiomyopathy on guideline-directed medical therapy. *Am. J. Cardiol.* 114:883–89
7. Masci PG, Schuurman R, Andrea B, et al. 2013. Myocardial fibrosis as a key determinant of left ventricular remodeling in idiopathic dilated cardiomyopathy. *Circ. Cardiovasc. Imaging* 6:790–99
8. Spieker M, Katsianos E, Gastl M, et al. 2018. T2 mapping cardiovascular magnetic resonance identifies the presence of myocardial inflammation in patients with dilated cardiomyopathy as compared to endomyocardial biopsy. *Eur. Heart J. Cardiovasc. Imaging* 19:574–82
9. Buss SJ, Breuninger K, Lehrke S, et al. 2015. Assessment of myocardial deformation with cardiac magnetic resonance strain imaging improves risk stratification in patients with dilated cardiomyopathy. *Eur. Heart J. Cardiovasc. Imaging* 16:307–15
10. Liang Y, Li W, Zeng R, et al. 2019. Left ventricular spherical index is an independent predictor for clinical outcomes in patients with nonischemic dilated cardiomyopathy. *JACC Cardiovasc. Imaging* 12:1578–80
11. Halliday BP, Wassall R, Lota AS, et al. 2019. Withdrawal of pharmacological treatment for heart failure in patients with recovered dilated cardiomyopathy (TRED-HF): an open-label, pilot, randomised trial. *Lancet* 393:61–73
12. Semsarian C, Ingles J, Maron MS, Maron BJ. 2015. New perspectives on the prevalence of hypertrophic cardiomyopathy. *J. Am. Coll. Cardiol.* 65:1249–54
13. Rudolph A, Abdel-Aty H, Bohl S, et al. 2009. Noninvasive detection of fibrosis applying contrast-enhanced cardiac magnetic resonance in different forms of left ventricular hypertrophy relation to remodeling. *J. Am. Coll. Cardiol.* 53:284–91
14. Ho CY, Abbasi SA, Neilan TG, et al. 2013. T1 measurements identify extracellular volume expansion in hypertrophic cardiomyopathy sarcomere mutation carriers with and without left ventricular hypertrophy. *Circ. Cardiovasc. Imaging* 6:415–22
15. Hinojar R, Varma N, Child N, et al. 2015. T1 mapping in discrimination of hypertrophic phenotypes: hypertensive heart disease and hypertrophic cardiomyopathy: findings from the International T1 Multicenter cardiovascular magnetic resonance study. *Circ. Cardiovasc. Imaging* 8:e003285
16. Raman B, Ariga R, Spartera M, et al. 2019. Progression of myocardial fibrosis in hypertrophic cardiomyopathy: mechanisms and clinical implications. *Eur. Heart J. Cardiovasc. Imaging* 20:157–67
17. Deva DP, Williams LK, Care M, et al. 2013. Deep basal inferoseptal crypts occur more commonly in patients with hypertrophic cardiomyopathy due to disease-causing myofilament mutations. *Radiology* 269:68–76
18. Maron MS, Olivotto I, Harrigan C, et al. 2011. Mitral valve abnormalities identified by cardiovascular magnetic resonance represent a primary phenotypic expression of hypertrophic cardiomyopathy. *Circulation* 124:40–47
19. Swoboda PP, McDiarmid AK, Erhayiem B, et al. 2016. Assessing myocardial extracellular volume by T1 mapping to distinguish hypertrophic cardiomyopathy from athlete's heart. *J. Am. Coll. Cardiol.* 67:2189–90
20. Martinez-Naharro A, Kotecha T, Norrington K, et al. 2018. Native T1 and extracellular volume in transthyretin amyloidosis. *JACC Cardiovasc. Imaging* 12:810–19
21. Karur GR, Robison S, Iwanochko RM, et al. 2018. Use of myocardial T1 mapping at 3.0 T to differentiate Anderson-Fabry disease from hypertrophic cardiomyopathy. *Radiology* 288:398–406
22. Weng Z, Yao J, Chan RH, et al. 2016. Prognostic value of LGE-CMR in HCM: a meta-analysis. *JACC Cardiovasc. Imaging* 9:1392–402

23. Shah JP, Yang Y, Chen S, et al. 2018. Prevalence and prognostic significance of right ventricular dysfunction in patients with hypertrophic cardiomyopathy. *Am. J. Cardiol.* 122:1932–38
24. Hinojar R, Zamorano JL, Fernandez-Mendez M, et al. 2019. Prognostic value of left atrial function by cardiovascular magnetic resonance feature tracking in hypertrophic cardiomyopathy. *Int. J. Cardiovasc. Imaging* 35:1055–65
25. Hinojar R, Fernandez-Golfin C, Gonzalez-Gomez A, et al. 2017. Prognostic implications of global myocardial mechanics in hypertrophic cardiomyopathy by cardiovascular magnetic resonance feature tracking. Relations to left ventricular hypertrophy and fibrosis. *Int. J. Cardiol.* 249:467–72
26. Hen Y, Takara A, Iguchi N, et al. 2018. High signal intensity on T2-weighted cardiovascular magnetic resonance imaging predicts life-threatening arrhythmic events in hypertrophic cardiomyopathy patients. *Circ. J.* 82:1062–69
27. Cheng S, Fang M, Cui C, et al. 2018. LGE-CMR-derived texture features reflect poor prognosis in hypertrophic cardiomyopathy patients with systolic dysfunction: preliminary results. *Eur. Radiol.* 28:4615–24
28. Vogelsberg H, Mahrholdt H, Deluigi CC, et al. 2008. Cardiovascular magnetic resonance in clinically suspected cardiac amyloidosis: noninvasive imaging compared to endomyocardial biopsy. *J. Am. Coll. Cardiol.* 51:1022–30
29. Banypersad SM, Sado DM, Flett AS, et al. 2013. Quantification of myocardial extracellular volume fraction in systemic AL amyloidosis: an equilibrium contrast cardiovascular magnetic resonance study. *Circ. Cardiovasc. Imaging* 6:34–39
30. Wan K, Sun J, Yang D, et al. 2018. Left ventricular myocardial deformation on cine MR images: relationship to severity of disease and prognosis in light-chain amyloidosis. *Radiology* 288:73–80
31. Wan K, Li W, Sun J, et al. 2019. Regional amyloid distribution and impact on mortality in light-chain amyloidosis: a T1 mapping cardiac magnetic resonance study. *Amyloid* 26:45–51
32. Kotecha T, Martinez-Naharro A, Treibel TA, et al. 2018. Myocardial edema and prognosis in amyloidosis. *J. Am. Coll. Cardiol.* 71:2919–31
33. Raina S, Lensing SY, Nairooz RS, et al. 2016. Prognostic value of late gadolinium enhancement CMR in systemic amyloidosis. *JACC Cardiovasc. Imaging* 9:1267–77
34. Wan K, Sun J, Han Y, et al. 2018. Increased prognostic value of query amyloid late enhancement score in light-chain cardiac amyloidosis. *Circ. J.* 82:739–46
35. Boynton SJ, Geske JB, Dispenzieri A, et al. 2016. LGE provides incremental prognostic information over serum biomarkers in AL cardiac amyloidosis. *JACC Cardiovasc. Imaging* 9:680–86
36. Wan K, Sun J, Han Y, et al. 2018. Right ventricular involvement evaluated by cardiac magnetic resonance imaging predicts mortality in patients with light chain amyloidosis. *Heart Vessels* 33:170–79
37. Illman JE, Arunachalam SP, Arani A, et al. 2018. MRI feature tracking strain is prognostic for all-cause mortality in AL amyloidosis. *Amyloid Int. J. Exp. Clin. Investig.* 25:101–8
38. Kouranos V, Tzelepis GE, Rapti A, et al. 2017. Complementary role of CMR to conventional screening in the diagnosis and prognosis of cardiac sarcoidosis. *JACC Cardiovasc. Imaging* 10:1437–47
39. Greulich S, Kitterer D, Latus J, et al. 2016. Comprehensive cardiovascular magnetic resonance assessment in patients with sarcoidosis and preserved left ventricular ejection fraction. *Circ. Cardiovasc. Imaging* 9:e005022
40. Puntmann VO, Isted A, Hinojar R, et al. 2017. T1 and T2 mapping in recognition of early cardiac involvement in systemic sarcoidosis. *Radiology* 285:63–72
41. Patel MR, Cawley PJ, Heitner JF, et al. 2009. Detection of myocardial damage in patients with sarcoidosis. *Circulation* 120:1969–77
42. Coleman GC, Shaw PW, Balfour PC Jr., et al. 2017. Prognostic value of myocardial scarring on CMR in patients with cardiac sarcoidosis. *JACC Cardiovasc. Imaging* 10:411–20
43. Carpenter JP, Roughton M, Pennell DJ. 2013. International survey of T2* cardiovascular magnetic resonance in beta-thalassemia major. *Haematologica* 98:1368–74
44. Casale M, Filosa A, Ragozzino A, et al. 2019. Long-term improvement in cardiac magnetic resonance in beta-thalassemia major patients treated with deferasirox extends to patients with abnormal baseline cardiac function. *Am. J. Hematol.* 94:312–18

45. Modell B, Khan M, Darlison M, et al. 2008. Improved survival of thalassaemia major in the UK and relation to T2* cardiovascular magnetic resonance. *J. Cardiovasc. Magn. Reson.* 10:42
46. Krittayaphong R, Zhang S, Saiviroonporn P, et al. 2017. Detection of cardiac iron overload with native magnetic resonance T1 and T2 mapping in patients with thalassemia. *Int. J. Cardiol.* 248:421–26
47. Basso C, Corrado D, Marcus FI, et al. 2009. Arrhythmogenic right ventricular cardiomyopathy. *Lancet* 373:1289–300
48. Marra MP, Leoni L, Bauce B, et al. 2012. Imaging study of ventricular scar in arrhythmogenic right ventricular cardiomyopathy: comparison of 3D standard electroanatomical voltage mapping and contrast-enhanced cardiac magnetic resonance. *Circ. Arrhythmia Electrophysiol.* 5:91–100
49. Te Riele AS, James CA, Philips B, et al. 2013. Mutation-positive arrhythmogenic right ventricular dysplasia/cardiomyopathy: the triangle of dysplasia displaced. *J. Cardiovasc. Electrophysiol.* 24:1311–20
50. Pfluger HB, Phrommintikul A, Mariani JA, et al. 2008. Utility of myocardial fibrosis and fatty infiltration detected by cardiac magnetic resonance imaging in the diagnosis of arrhythmogenic right ventricular dysplasia—a single centre experience. *Heart Lung Circ.* 17:478–83
51. Tandri H, Saranathan M, Rodriguez ER, et al. 2005. Noninvasive detection of myocardial fibrosis in arrhythmogenic right ventricular cardiomyopathy using delayed-enhancement magnetic resonance imaging. *J. Am. Coll. Cardiol.* 45:98–103
52. Petersen SE, Selvanayagam JB, Wiesmann F, et al. 2005. Left ventricular non-compaction: insights from cardiovascular magnetic resonance imaging. *J. Am. Coll. Cardiol.* 46:101–5
53. Jacquier A, Thuny F, Jop B, et al. 2010. Measurement of trabeculated left ventricular mass using cardiac magnetic resonance imaging in the diagnosis of left ventricular non-compaction. *Eur. Heart J.* 31:1098–104
54. Japp AG, Gulati A, Cook SA, et al. 2016. The diagnosis and evaluation of dilated cardiomyopathy. *J. Am. Coll. Cardiol.* 67:2996–3010
55. Amzulescu MS, Rousseau MF, Ahn SA, et al. 2015. Prognostic impact of hypertrabeculation and non-compaction phenotype in dilated cardiomyopathy: a CMR study. *JACC Cardiovasc. Imaging* 8:934–46
56. Paetsch I, Jahnke C, Wahl A, et al. 2004. Comparison of dobutamine stress magnetic resonance, adenosine stress magnetic resonance, and adenosine stress magnetic resonance perfusion. *Circulation* 110:835–42
57. Karamitsos TD, Ntusi NA, Francis JM, et al. 2010. Feasibility and safety of high-dose adenosine perfusion cardiovascular magnetic resonance. *J. Cardiovasc. Magn. Reson.* 12:66
58. Kiaos A, Tziatzios I, Hadjimiltiades S, et al. 2018. Diagnostic performance of stress perfusion cardiac magnetic resonance for the detection of coronary artery disease: a systematic review and meta-analysis. *Int. J. Cardiol.* 252:229–33
59. Nandalur KR, Dwamena BA, Choudhri AF, et al. 2007. Diagnostic performance of stress cardiac magnetic resonance imaging in the detection of coronary artery disease: a meta-analysis. *J. Am. Coll. Cardiol.* 50:1343–53
60. Gargiulo P, Dellegrottaglie S, Bruzzese D, et al. 2013. The prognostic value of normal stress cardiac magnetic resonance in patients with known or suspected coronary artery disease: a meta-analysis. *Circ. Cardiovasc. Imaging* 6:574–82
61. Heitner JF, Kim RJ, Kim HW, et al. 2019. Prognostic value of vasodilator stress cardiac magnetic resonance imaging: a multicenter study with 48 000 patient-years of follow-up. *JAMA Cardiol.* 4:256–64
62. Miller CD, Case LD, Little WC, et al. 2013. Stress CMR reduces revascularization, hospital readmission, and recurrent cardiac testing in intermediate-risk patients with acute chest pain. *JACC Cardiovasc. Imaging* 6:785–94
63. Jekic M, Foster EL, Ballinger MR, et al. 2008. Cardiac function and myocardial perfusion immediately following maximal treadmill exercise inside the MRI room. *J. Cardiovasc. Magn. Reson.* 10:3
64. Raman SV, Dickerson JA, Jekic M, et al. 2010. Real-time cine and myocardial perfusion with treadmill exercise stress cardiovascular magnetic resonance in patients referred for stress SPECT. *J. Cardiovasc. Magn. Reson.* 12:41
65. Sukpraphrute B, Drafts BC, Rerkpattanapipat P, et al. 2015. Prognostic utility of cardiovascular magnetic resonance upright maximal treadmill exercise testing. *J. Cardiovasc. Magn. Reson.* 17:103

66. Romero J, Xue X, Gonzalez W, Garcia MJ. 2012. CMR imaging assessing viability in patients with chronic ventricular dysfunction due to coronary artery disease: a meta-analysis of prospective trials. *JACC Cardiovasc. Imaging* 5:494–508
67. Selvanayagam JB, Kardos A, Francis JM, et al. 2004. Value of delayed-enhancement cardiovascular magnetic resonance imaging in predicting myocardial viability after surgical revascularization. *Circulation* 110:1535–41
68. Gutberlet M, Frohlich M, Mehl S, et al. 2005. Myocardial viability assessment in patients with highly impaired left ventricular function: comparison of delayed enhancement, dobutamine stress MRI, end-diastolic wall thickness, and TI201-SPECT with functional recovery after revascularization. *Eur. Radiol.* 15:872–80
69. Gerber BL, Rousseau MF, Ahn SA, et al. 2012. Prognostic value of myocardial viability by delayed-enhanced magnetic resonance in patients with coronary artery disease and low ejection fraction: impact of revascularization therapy. *J. Am. Coll. Cardiol.* 59:825–35
70. Liu D, Borlotti A, Viliani D, et al. 2017. CMR native T1 mapping allows differentiation of reversible versus irreversible myocardial damage in ST-segment-elevation myocardial infarction: an OxAMI study (Oxford Acute Myocardial Infarction). *Circ. Cardiovasc. Imaging* 10:e005986
71. Kato S, Kitagawa K, Ishida N, et al. 2010. Assessment of coronary artery disease using magnetic resonance coronary angiography: a national multicenter trial. *J. Am. Coll. Cardiol.* 56:983–91
72. Wilensky RL, Song HK, Ferrari VA. 2006. Role of magnetic resonance and intravascular magnetic resonance in the detection of vulnerable plaques. *J. Am. Coll. Cardiol.* 47:C48–56
73. Rashid I, Maghzal GJ, Chen YC, et al. 2018. Myeloperoxidase is a potential molecular imaging and therapeutic target for the identification and stabilization of high-risk atherosclerotic plaque. *Eur. Heart J.* 39:3301–10
74. Agewall S, Beltrame JF, Reynolds HR, et al. 2017. ESC working group position paper on myocardial infarction with non-obstructive coronary arteries. *Eur. Heart J.* 38:143–53
75. Assomull RG, Lyne JC, Keenan N, et al. 2007. The role of cardiovascular magnetic resonance in patients presenting with chest pain, raised troponin, and unobstructed coronary arteries. *Eur. Heart J.* 28:1242–49
76. Pathik B, Raman B, Mohd Amin NH, et al. 2016. Troponin-positive chest pain with unobstructed coronary arteries: incremental diagnostic value of cardiovascular magnetic resonance imaging. *Eur. Heart J. Cardiovasc. Imaging* 17:1146–52
77. Rodrigues P, Joshi A, Williams H, et al. 2017. Diagnosis and prognosis in sudden cardiac arrest survivors without coronary artery disease: utility of a clinical approach using cardiac magnetic resonance imaging. *Circ. Cardiovasc. Imaging* 10:e006709
78. Habibi M, Samiei S, Ambale Venkatesh B, et al. 2016. Cardiac magnetic resonance-measured left atrial volume and function and incident atrial fibrillation: results from MESA (Multi-Ethnic Study of Atherosclerosis). *Circ. Cardiovasc. Imaging* 9(8):e004299
79. Marrouche NF, Wilber D, Hindricks G, et al. 2014. Association of atrial tissue fibrosis identified by delayed enhancement MRI and atrial fibrillation catheter ablation: the DECAAF study. *JAMA* 311:498–506
80. Bisbal F, Guiu E, Cabanas-Grandio P, et al. 2014. CMR-guided approach to localize and ablate gaps in repeat AF ablation procedure. *JACC Cardiovasc. Imaging* 7:653–63
81. Dukkipati SR, Sanz J. 2014. Contrast-enhanced CMR imaging of ventricular tachycardia isthmus sites to guide ablation: an approach in evolution. *JACC Cardiovasc. Imaging* 7:785–87
82. Andreu D, Ortiz-Perez JT, Boussy T, et al. 2014. Usefulness of contrast-enhanced cardiac magnetic resonance in identifying the ventricular arrhythmia substrate and the approach needed for ablation. *Eur. Heart J.* 35:1316–26
83. Paetsch I, Sommer P, Jahnke C, et al. 2019. Clinical workflow and applicability of electrophysiological cardiovascular magnetic resonance-guided radiofrequency ablation of isthmus-dependent atrial flutter. *Eur. Heart J. Cardiovasc. Imaging* 20:147–56
84. Altmayer SP, Patel AR, Addetia K, et al. 2016. Cardiac MRI right ventricle/left ventricle (RV/LV) volume ratio improves detection of RV enlargement. *J. Magn. Reson. Imaging* 43:1379–85

85. Sanz J, Kuschnir P, Rius T, et al. 2007. Pulmonary arterial hypertension: noninvasive detection with phase-contrast MR imaging. *Radiology* 243:70–79
86. Freed BH, Gomberg-Maitland M, Chandra S, et al. 2012. Late gadolinium enhancement cardiovascular magnetic resonance predicts clinical worsening in patients with pulmonary hypertension. *J. Cardiovasc. Magn. Reson.* 14:11
87. Chen YY, Yun H, Jin H, et al. 2017. Association of native T1 times with biventricular function and hemodynamics in precapillary pulmonary hypertension. *Int. J. Cardiovasc. Imaging* 33:1179–89
88. Sanz J, Kariisa M, Dellegrottaglie S, et al. 2009. Evaluation of pulmonary artery stiffness in pulmonary hypertension with cardiac magnetic resonance. *JACC Cardiovasc. Imaging* 2:286–95
89. Rodes-Cabau J, Domingo E, Roman A, et al. 2003. Intravascular ultrasound of the elastic pulmonary arteries: a new approach for the evaluation of primary pulmonary hypertension. *Heart* 89:311–15
90. Reiter G, Reiter U, Kovacs G, et al. 2015. Blood flow vortices along the main pulmonary artery measured with MR imaging for diagnosis of pulmonary hypertension. *Radiology* 275:71–79
91. Myerson SG. 2012. Heart valve disease: investigation by cardiovascular magnetic resonance. *J. Cardiovasc. Magn. Reson.* 14:7
92. Dweck MR, Joshi S, Murigu T, et al. 2011. Midwall fibrosis is an independent predictor of mortality in patients with aortic stenosis. *J. Am. Coll. Cardiol.* 58:1271–79
93. Chin CWL, Everett RJ, Kwiecinski J, et al. 2017. Myocardial fibrosis and cardiac decompensation in aortic stenosis. *JACC Cardiovasc. Imaging* 10:1320–33
94. Wang J, Jagasia DH, Kondapally YR, et al. 2017. Comparison of non-contrast cardiovascular magnetic resonance imaging to computed tomography angiography for aortic annular sizing before transcatheter aortic valve replacement. *J. Invasive Cardiol.* 29:239–45
95. Lerakis S, Hayek S, Arepalli CD, et al. 2014. Cardiac magnetic resonance for paravalvular leaks in post-transcatheter aortic valve replacement. *Circulation* 129:e430–31
96. Zoghbi WA, Adams D, Bonow RO, et al. 2017. Recommendations for noninvasive evaluation of native valvular regurgitation: a report from the American Society of Echocardiography developed in collaboration with the Society for Cardiovascular Magnetic Resonance. *J. Am. Soc. Echocardiogr.* 30:303–71
97. Cawley PJ, Hamilton-Craig C, Owens DS, et al. 2013. Prospective comparison of valve regurgitation quantitation by cardiac magnetic resonance imaging and transthoracic echocardiography. *Circ. Cardiovasc. Imaging* 6:48–57
98. Penicka M, Vecera J, Mirica DC, et al. 2018. Prognostic implications of magnetic resonance-derived quantification in asymptomatic patients with organic mitral regurgitation: comparison with Doppler echocardiography-derived integrative approach. *Circulation* 137:1349–60
99. Han Y, Peters DC, Salton CJ, et al. 2008. Cardiovascular magnetic resonance characterization of mitral valve prolapse. *JACC Cardiovasc. Imaging* 1:294–303
100. Oosterhof T, van Straten A, Vliegen HW, et al. 2007. Preoperative thresholds for pulmonary valve replacement in patients with corrected tetralogy of Fallot using cardiovascular magnetic resonance. *Circulation* 116:545–51